

Morphological Effects of Microphase Separation on the Permselectivity for Aqueous Ethanol Solutions of Block and Graft Copolymer Membranes Containing Poly(dimethylsiloxane)

Takashi Miyata,* Seiji Obata, and Tadashi Uragami*

Chemical Branch, Faculty of Engineering and High Technology Research Center, Kansai University, Suita, Osaka 564-8680, Japan

Received December 18, 1998

ABSTRACT: The permselectivity of block copolymer membranes consisting of ethanol-permselective poly-(dimethylsiloxane) (PDMS) plus water-permselective poly(methyl methacrylate) (PMMA) was compared to the permselectivity of graft copolymer membranes for the separation of an aqueous ethanol solution. This paper focuses on the difference in molecular architecture between the block and graft copolymers and relates microphase separation in these membranes to their permeability and permselectivity for an aqueous ethanol solution in pervaporation. With increasing DMS content, the block copolymer membranes changed from water- to ethanol-permselective at a DMS content of 55 mol %. As reported in a previous paper, however, the graft copolymer membranes showed a dramatic change in the permselectivity at a DMS content of 35 mol %. Transmission electron micrography demonstrated that both membranes had distinct microphase separation consisting of PDMS and PMMA phases and that the morphology was quite different between the block and graft copolymer membranes. The morphological changes in these membranes were investigated by image processing of the micrographs and analysis using a combined model consisting of both parallel and series models. These investigations revealed that the percolation transition of the PDMS phase in the block and graft copolymer membranes takes place at a DMS content of about 55 and 35 mol %, respectively. This suggests that the continuity of the PDMS phase in the microphase separation strongly influences the ethanol permselectivity of these membranes for an aqueous ethanol solution. This report concludes that the design of the molecular architecture in multicomponent polymer membranes is very important in controlling membrane characteristics which are governed by microphase separation.

Introduction

The separation of organic liquid mixtures such as alcohol/water, benzene/cyclohexane, etc., has become increasingly important because of their high potential as valuable fuels and raw materials. However, these mixtures cannot be completely separated by the distillation method because of azeotropes and close boiling points. Membrane techniques have many advantages in terms of potential savings in energy costs for the separation of such mixtures. In particular, pervaporation is a highly promising technique for the separation of organic liquid mixtures.¹ Many studies have been reported on the development of pervaporation membranes for the separation of aqueous ethanol solutions, as the separation of ethanol and water is very important for the commercial production of alcohol. Pervaporation membranes for the separation of aqueous ethanol solutions can be divided into water- and ethanol-permselective membranes, which preferentially permeate water and ethanol, respectively. Poly(dimethylsiloxane) (PDMS), poly[1-(trimethylsilyl)-1-propyne] (PTMSP), and their derivative membranes are representative ethanol-permselective membranes,^{2–7} whereas most of the other membranes are water-permselective.^{8,9} The permeability and permselectivity of pervaporation membranes are mainly governed by the solubility and the diffusivity of the permeants in the membranes. For example, the ethanol-permselective membranes preferentially permeate ethanol due to their stronger affinity for ethanol than for water and to the relatively high diffusivity of ethanol through these membranes.

Multicomponent polymers have attracted considerable attention in the industrial field, since these compounds combine a variety of functional components into a single material.^{10–14} In most multicomponent polymers, micro- or macrophase separation often takes place due to the very small entropy and positive heat of mixing. Since these phase-separated structures directly affect the physical and chemical properties of the polymer, the morphology of the polymer phase separation must be controlled in developing a high-performance polymer. In addition, naturally phase-separated structures in multicomponent polymer membranes strongly govern their permeability and permselectivity. Some researchers have studied the relationship between the phase-separated morphology of multicomponent polymer membranes and their gas permeation with a variety of models.^{15–27} On the other hand, only a few reports have described the effects of microphase separation on membrane permselectivity in pervaporation membranes for the separation of organic liquid mixtures.^{28–31} Kerres et al.²⁸ reported that morphological changes in multicomponent polymer membranes caused a drastic change in their permselectivity at the percolation point. It is very important to examine the relationship between microphase separation and permselectivity for organic liquid mixtures in pervaporation membranes by the application of various structural models, because microphase separation has a more marked influence on permeability and permselectivity in pervaporation membranes than in gas permeation membranes.

We have studied the relationship between the structure and properties of multicomponent polymer membranes in order to develop high-performance pervapo-

* To whom correspondence should be addressed.

ration membranes for the separation of aqueous ethanol solutions.^{29–34} For example, adding block or graft copolymers containing fluorine into the ethanol-permselective membranes enabled us to control their surface properties and resulted in improving the ethanol permselectivity.^{32–34} Other projects have focused on the microphase separation in multicomponent polymer membranes consisting of ethanol- and water-permselective components. It was apparent from our previous studies that the permeability and permselectivity of graft copolymer membranes containing PDMS were strongly dependent upon the morphology of their microphase separation.^{29,30} These investigations into multicomponent pervaporation membranes have contributed significantly to our understanding of the permeation mechanisms of pervaporation.

Similar to graft copolymers, most block copolymers are phase-separated, but the morphologies of the domains in the phase separation, such as their size or shape, are quite different between block and graft copolymers. This is due to the difference in the molecular architecture between graft and block copolymers. The morphologies of the block copolymers have been modeled by Molau.³⁵ For example, as the content of the A component in an AB diblock copolymers increases, the morphology transforms from A spheres to A cylinders, then to AB lamellae, and back to B cylinders and B spheres of the inverse morphology. Sometimes, block copolymers can be more regular than the equivalent graft copolymers. Therefore, it is very interesting to relate the morphology of block copolymer membranes to their permeability and permselectivity. Furthermore, fundamental research on the microphase separation and permselectivity of multicomponent polymer membranes by comparing block versus graft copolymer membranes will lead to a better understanding of the pervaporation process during the separation of organic liquid mixtures.

The purpose of our studies was to determine the relationship between the morphology of the microphase separation in two-component polymer membranes consisting of ethanol- and water-permselective components and their permeability and permselectivity for aqueous ethanol solutions during pervaporation. In particular, the effects of the microphase separation on the permeability and permselectivity of block copolymer membranes were compared to those of graft copolymer membranes. Block and graft copolymer membranes consisting of ethanol-permselective PDMS and water-permselective PMMA were prepared by the polymerization of methyl methacrylate (MMA) with a PDMS macro-azo-initiator and by the copolymerization of MMA with a PDMS macromonomer, respectively, according to methods previously reported.^{29–34} The results of pervaporation for an aqueous ethanol solution through two types of copolymer membranes consisting of the same components were evaluated in more detail from the perspective of the morphological changes in block and graft copolymer membranes.

Experimental Section

Materials. The poly(dimethylsiloxane) (PDMS) macro-azo-initiator (PASA) (1),^{36–38} which has 59 units of the PDMS block subunit, was supplied by Wako Pure Chemical Industries, Ltd. The PDMS macromonomer (2), which has 81 units of the pendant PDMS, was supplied by Toray Dow Corning Silicone Co., Ltd. Methyl methacrylate (MMA) monomer was purified by distillation under reduced pressure in nitrogen gas. All other solvents and reagents were of analytical grade and were

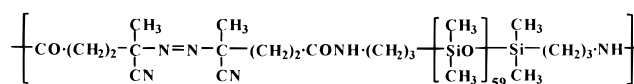
Table 1. Results of the Polymerization of MMA with a PDMS Macroinitiator

feed DMS units (mol %)	molecular weight ^a			polymer ^b DMS units (mol %)
	M_w	M_n	M_w/M_n	
0	89 000	51 000	1.75	0
30	175 000	105 000	1.67	29
40	172 000	105 000	1.64	35
45	150 000	112 000	1.34	41
60	135 000	100 000	1.35	54
65	113 000	66 000	1.70	59
70	106 000	66 000	1.60	62
80	112 000	55 000	2.05	73

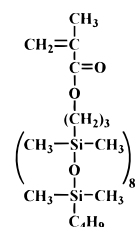
^a Determined by GPC calibrated with polystyrene standard.

^b Determined by ¹H NMR.

obtained from commercial sources and used without further purification.



PDMS macro-azo-initiator (1)



PDMS macromonomer (2)

Synthesis of Block and Graft Copolymers. PDMS macroinitiator and MMA in a typical composition were dissolved in benzene to create a 40 wt % solution, and the mixture was then transferred to a glass tube. The polymerization was carried out at 60 °C for 6 h under nitrogen gas. The resulting block copolymer (PMMA-*b*-PDMS) was isolated by slow precipitation with a 1:2 mixture of *n*-hexane and ethanol. The copolymer was purified by reprecipitation from the benzene solution into a 1:2 mixture of *n*-hexane and ethanol and then dried at 40 °C in vacuo.

The average molecular weight of PMMA-*b*-PDMS was determined by a gel permeation chromatograph (GPC) (Waters Associate Inc.; R-400), equipped with a TSK-GEL column (Tosoh Co. Ltd.; G2000HXL, G3000HXL, G5000HXL) and ultraviolet spectrophotometry (Shimadzu Co. Ltd.; SPD-2A). Tetrahydrofuran was used as an eluant, and the calibration was performed with polystyrene standards. The number-average molecular weights of PMMA-*b*-PDMS ranged from about 50 000 to 110 000 g/mol. The ratio of the weight-average molecular weight to the number-average molecular weight (M_w/M_n) was less than two.

The composition of the resultant PMMA-*b*-PDMS was determined from the 270 MHz ¹H nuclear magnetic resonance (NMR) (JEOL; GSX-270) spectra obtained by measuring the integrals of the peaks assigned to the methyl protons (3.5 ppm) of the PMMA component, and the dimethylsiloxane protons (0 ppm) of the PDMS component, after the purified copolymer had been dissolved in chloroform-*d*. The DMS content of the PMMA-*b*-PDMS was slightly lower than that in the feed. The characterization of the PMMA-*b*-PDMS copolymer is summarized in Table 1.

Graft copolymers consisting of PDMS and PMMA (PMMA-*g*-PDMS) were synthesized by the copolymerization of the PDMS macromonomer with MMA by the methods reported in a previous paper.^{29,30} The composition and average molec-

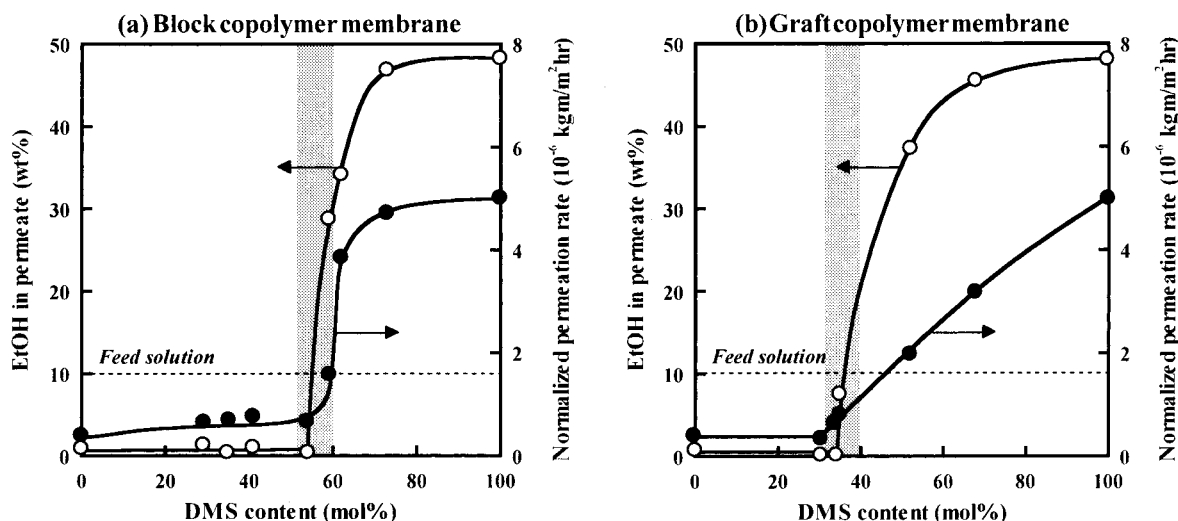


Figure 1. Effects of the DMS content on the ethanol concentration of the permeate (○) and on the normalized permeation rate (●) through PMMA-*b*-PDMS (a) and PMMA-*g*-PDMS (b) membranes during pervaporation. The feed solution was an aqueous solution of 10 wt % ethanol (40 °C). The dashed line represents the feed composition.

ular weights of the resultant PMMA-*g*-PDMS have been reported in the previous paper.

Membrane Preparation. The prescribed amounts of PMMA-*b*-PDMS and PMMA-*g*-PDMS were dissolved in benzene at 25 °C to a concentration of 4 wt % for the preparation of the casting solutions. The PMMA-*b*-PDMS and PMMA-*g*-PDMS membranes were prepared by pouring the casting solutions onto rimmed glass plates and then allowing the solvent to evaporate completely at 25 °C. The resultant membranes were transparent, and their thickness was about 40 μ m.

Glass Transition Temperature Measurements. The glass transition temperatures (T_g 's) of the PMMA-*b*-PDMS membranes were determined by differential scanning calorimetry (DSC) (Rigaku; TAS-200). The specimens were heated from about -160 to 180 °C, with a heating rate of 20 °C/min.

Transmission Electron Micrographs (TEM). The PMMA-*b*-PDMS membranes were vapor-stained with an aqueous solution of 5 wt % RuO₄ in glass-covered dishes.³⁹ The stained membranes were then embedded in epoxy resin and cross sectioned into thin films (thickness: approximately 60 nm) with a microtome (Leica; Reichert Ultracut E). The morphological features that were highlighted by our staining procedure were observed with a transmission electron microscope (TEM) (JEOL JEM-1210) at an accelerating voltage of 80 kV.

Permeation Measurements. The pervaporation was performed using the apparatus described in a previous paper.²⁹⁻³⁴ under the following conditions: permeation temperature, 40 °C; pressure on the permeate side, 1×10^{-2} Torr. The effective membrane area was 13.8 cm². In all pervaporation experiments of this study, the air side surfaces of the PMMA-*b*-PDMS and PMMA-*g*-PDMS membranes were exposed to the feed side of the permeation cell. An aqueous solution of 10 wt % ethanol was used as the feed solution. The compositions of the feed solution and permeate were determined by a gas chromatograph (Shimadzu GC-9A) equipped with a flame ionization detector (FID) and a capillary column (Shimadzu Co. Ltd.; Shimalite F) heated to 200 °C. The permeation rates of an aqueous ethanol solution during pervaporation were determined from the weight of the permeate collected in a cold trap, the permeation time, and the effective membrane area. The results of the permeation of an aqueous ethanol solution by pervaporation were reproducible, and the errors inherent in the permeation measurements were of the order of a few percent.

Results and Discussion

Pervaporation Characteristics of PMMA-*b*-PDMS and PMMA-*g*-PDMS Membranes.

Figure 1 shows the

effects of the DMS content of the PMMA-*b*-PDMS and PMMA-*g*-PDMS membranes on the ethanol concentration in the permeate and on the normalized permeation rate of an aqueous solution of 10 wt % ethanol through the membranes. In this figure, the normalized permeation rate which is the product of the permeation rate and the membrane thickness is used for evaluating the essential permeability of the membrane. The normalization of the permeation rate can reveal the detailed relationship between the membrane structure and the permeability. The normalized permeation rate through the PMMA-*b*-PDMS membrane was constant at about 0.5×10^{-6} kg/(m² h) up to a DMS content of 55 mol % and then increased dramatically with increases in the DMS content over 55 mol %. A PDMS membrane has the generally higher diffusivity than glassy polymer membranes except polysilylated propyne membranes due to high mobility of its polymer chain and high free volume rubbers.^{40,41} The much higher diffusivity in the PDMS component causes an increase in the normalized permeation rate with increasing DMS content. The ethanol concentration of the permeate passing through a PMMA-*b*-PDMS membrane with a DMS content of less than 55 mol % was generally less than 10 wt %. This suggests that membranes with a DMS content of less than 55 mol % are water-permselective. With increasing DMS contents over 55 mol %, however, the ethanol concentration in the permeate increased dramatically over 10 wt %. Therefore, PMMA-*b*-PDMS membranes with a DMS content of more than 55 mol % became ethanol-permselective. PMMA and PDMS homopolymer membranes show strong water and ethanol permselectivity, respectively. Consequently, the PMMA-*b*-PDMS membrane changes from water to ethanol permselectivity upon an increase in the ethanol-permselective PDMS component. On the other hand, as reported in previous papers,^{29,30} the PMMA-*g*-PDMS membrane showed an abrupt increase in both the ethanol concentration of the permeate and the normalized permeation rate at a DMS content of about 35 mol %. The DMS content at which the PMMA-*b*-PDMS membranes change from water- to ethanol-permselective is quite different from that of the PMMA-*g*-PDMS membranes. It is quite obvious that the PMMA-*b*-PDMS membranes are water-permselective whereas the PMMA-

Table 2. Glass Transition Temperatures (T_g 's) of PMMA-*b*-PDMS Membranes with Various DMS Contents

DMS content (mol%)		T_g (°C)	
feed	polymer	high	low
0	0	128	
30	29	115	-131
40	35	116	-129
45	41	116	-134
60	54	117	-133
70	62	119	-134
80	73	121	-132
100	100		-127

g-PDMS membranes are ethanol-permselective at a DMS content between 35 and 55 mol %. Therefore, the permselectivity of membranes with a DMS content between 35 and 55 mol % is quite different between block and graft copolymer membranes. These results suggest that the permeability and permselectivity of multicomponent polymer membranes containing PDMS can be controlled by changing their molecular architecture without changing the polymer composition. To determine the reason why the DMS content at which the membrane properties changed was quite different between block and graft copolymer membranes, we focused on the differences in membrane structure in the next section.

Morphology of the Microphase Separation. Multicomponent polymer membranes often have a heterogeneous structure because of the immiscibility of each component. T_g measurements obtained by DSC enabled us to investigate the heterogeneity of a membrane. Table 2 shows the glass transition temperatures (T_g 's) of PMMA-*b*-PDMS membranes with various DMS contents. Two T_g 's were observed at about 120 and -130 °C in all block copolymer membranes. The fact that the T_g 's of the PMMA and PDMS homopolymers were 128 and -127 °C, respectively, suggests that the higher T_g in the block copolymer membranes was due to the PMMA component and the lower T_g from the PDMS component. The presence of two T_g 's in all block copolymer membranes implies that the membranes had a heterogeneous structure. On the other hand, as reported in previous papers,^{29,30} PMMA-*g*-PDMS membranes also have a higher T_g assigned to the PMMA component and a lower T_g assigned to the PDMS component. There are very few differences in the T_g 's between PMMA-*b*-PDMS and PMMA-*g*-PDMS membranes. The fact that the PMMA-*b*-PDMS membranes have two T_g 's such as the PMMA-*g*-PDMS membranes implies that the PMMA-*b*-PDMS membranes have a heterogeneous structure similar to the PMMA-*g*-PDMS membranes.

Figure 2 shows the transmission electron micrographs from a cross section of PMMA-*b*-PDMS membranes with various DMS contents. On these micrographs, only the PDMS component was stained by the RuO₄. These TEM pictures clearly demonstrated that all of the PMMA-*b*-PDMS membranes had distinct microphase separations consisting of PMMA and PDMS phases. This supports the results of the T_g measurements. The morphology of the microphase separation is strongly dependent upon the DMS content. In particular, the morphology of membranes with a DMS content of more than 59 mol % was quite different from those with a DMS content of less than 41 mol %. In a previous study,³⁰ we showed TEM images obtained from PMMA-*g*-PDMS membranes: the TEM images of the PMMA-*b*-PDMS membranes shown in Figure 2 are quite different from the

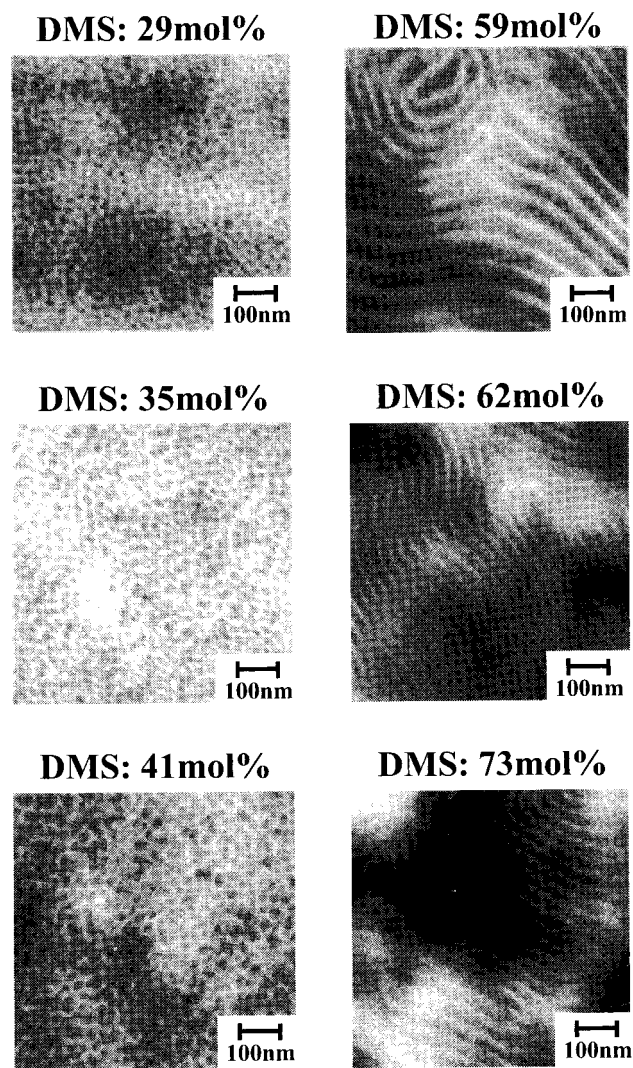


Figure 2. Transmission electron micrographs of cross sections of PMMA-*b*-PDMS membranes with various DMS contents. The dark region stained by RuO₄ represents the PDMS component.

PMMA-*g*-PDMS membranes shown in the previous paper. In the PMMA-*g*-PDMS membrane, the dispersed PDMS phase became larger with increasing DMS content, and it appeared that the PDMS component in the PMMA-*g*-PDMS membranes formed a continuous phase at a DMS content of more than 35 mol %. In the PMMA-*b*-PDMS membranes, however, membranes with a DMS content of less than about 55 mol % had a microphase separation consisting of a discontinuous PDMS phase and a continuous PMMA phase. Increasing the DMS content in the PMMA-*b*-PDMS membranes resulted in enlarging the PDMS phase until it formed a continuous phase at a DMS content of about 55 mol %. As a result, PMMA-*b*-PDMS membranes with a DMS content of more than 55 mol % have bicontinuous PDMS and PMMA phases, as shown in Figure 2.

The DMS content at which the morphology of the microphase separation changed dramatically was also quite different between the PMMA-*b*-PDMS and PMMA-*g*-PDMS membranes. It is worth noting that the DMS content at which the permeability and permselectivity changed remarkably in both PMMA-*b*-PDMS and PMMA-*g*-PDMS membranes was very similar to the DMS content for the morphological changes. This suggests that their permeability and permselectivity were mainly

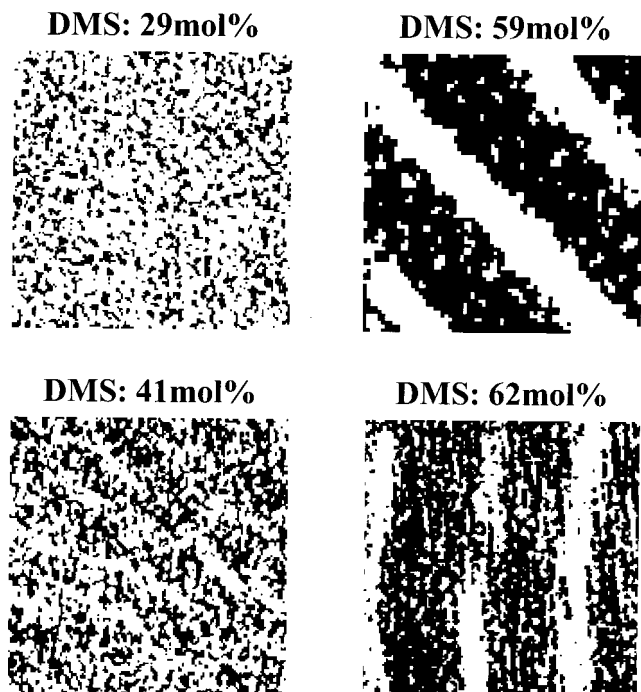


Figure 3. Image processing of transmission electron micrographs of the PMMA-*b*-PDMS membranes.

governed by the morphology of the microphase separation. It is likely that the morphological changes of the PDMS phase strongly influence other membrane characteristics.

A previous study³⁰ has demonstrated that image processing for TEM micrographs is very useful in analyzing the morphological changes of the microphase separation. Therefore, image processing of the TEM micrographs of the PMMA-*b*-PDMS membranes was performed for a more detailed investigation of the morphology according to the method previously reported. Briefly, the TEM image was transferred to a personal computer, and small PDMS clusters made up of less than 12 pixels were eliminated whereas larger PDMS clusters were left by the image processing. The results of image processing for the microphase separation in PMMA-*b*-PDMS membranes are shown in Figure 3. It is apparent that the PDMS clusters grew gradually as the DMS content increased. In PMMA-*b*-PDMS membranes with a DMS content of 29 and 41 mol %, a number of PDMS clusters of finite size (PDMS clusters made up of a few pixels) existed. However, when the DMS content increased to over 59 mol %, enormous PDMS clusters formed a continuous phase in the direction of the membrane thickness. The image processing demonstrated that the percolation transition of the PDMS phase takes place at a DMS content of about 55 mol %. The percolation point of the PMMA-*b*-PDMS membranes was consistent with the DMS content at which the membrane characteristics changed dramatically. Keres et al.²⁸ reported that a copolymer microphase inversion takes place at a percolation point in the region of a PDMS volume fraction of 0.36. The previous study on the morphology of the PMMA-*g*-PDMS membrane also reported that the percolation transition of the PDMS phase occurred at a DMS content of about 40 mol %. However, the percolation point of the PMMA-*b*-PDMS membrane is quite different from that of the PMMA-*g*-PDMS membrane reported in the previous papers. This is due to the fact

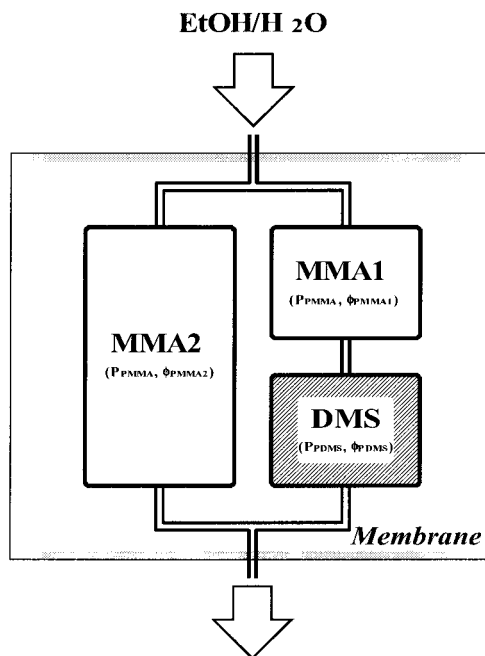


Figure 4. Schematic representation of the combined model consisting of both a series model and a parallel model.

that the PDMS component in a block copolymer forms a continuous phase with much greater difficulty than in a graft copolymer. In other words, the differences in the molecular architecture between graft and block copolymers strongly influence the morphological changes in the microphase separation of copolymer membranes.

Structural Models for Permeability. The properties of a membrane consisting of glassy and rubbery components are strongly dependent on the arrangement of the glassy and rubbery phases. For example, Tsujita et al.²¹ discussed the relationship between the DMS content and the permeability of CO₂ through microphase-separated, siloxane-imide block copolymer membranes based on two types of two-phase models: a parallel model and a series model. In the former, the two phases are arranged parallel to the direction of the permeation. The latter model has a structure in which the two phases are arranged perpendicular to the direction of permeation. The total permeability in the parallel model, consisting of phase A and phase B, can be represented by eq 1:

$$P = \phi_A P_A + \phi_B P_B \quad (1)$$

where ϕ_i and P_i are the volume fraction and the normalized permeation rate for phase i , respectively. In the series model, the total permeability is related to the permeability and volume fraction for each phase, as outlined by eq 2:

$$\frac{1}{P} = \frac{\phi_A}{P_A} + \frac{\phi_B}{P_B} \quad (2)$$

On the basis of these models, a combined model consisting of a series model plus a parallel model can be developed (Figure 4). In the combined model, the PMMA phase is divided into a PMMA1 phase in series and a PMMA2 phase in parallel. The PDMS phase is arranged in series with the PMMA1 phase and parallel to the PMMA2 phase. The total normalized permeation rate (P) in the combined model is given by eq 3:

$$P = (\phi_{\text{PDMS}} + \phi_{\text{PMMA1}}) \frac{P_{\text{PMMA}} P_{\text{PDMS}}}{\phi_{\text{PDMS}} P_{\text{PMMA}} + \phi_{\text{PMMA1}} P_{\text{PDMS}} + \phi_{\text{PMMA2}} P_{\text{PMMA}}} + \phi_{\text{PMMA1}} + \phi_{\text{PMMA2}} + \phi_{\text{PDMS}} = 1 \quad (3)$$

The purpose of this section is to quantitatively follow the morphological changes in microphase separation as a function of the DMS content. The volume fraction of each phase in the combined model is useful in quantitatively analyzing the morphological changes of the microphase separation. Therefore, we determined the volume fraction of each phase (ϕ_{PMMA1} , ϕ_{PMMA2} , ϕ_{PDMS}) from the experimental normalized permeation rates (P , P_{PMMA} , P_{PDMS}) of an aqueous ethanol solution using eq 3. The results for PMMA-*b*-PDMS and PMMA-*g*-PDMS membranes are shown in Figure 5. No effect of the swelling of the PMMA-*b*-PDMS and PMMA-*g*-PDMS membranes on the combined model needs to be considered because the membranes were very little swollen in an aqueous ethanol solution. Predictably, the calculated volume fraction of the PDMS phase increased with the DMS content in both membranes. More remarkable is the change in the volume fraction of the PMMA1 phase, which is arranged in series with the PDMS phase. In both membranes, the volume fraction of the PMMA1 phase showed a sharp decrease with increasing DMS content. The volume fraction of the PMMA1 phase in the PMMA-*g*-PDMS membranes decreased dramatically at a DMS content above 40 mol %, but the volume fraction in the PMMA-*b*-PDMS approaches zero at over 60 mol %. Furthermore, the volume fraction of the PMMA2 phase, which is arranged in parallel with the PDMS phase, increased abruptly in both PMMA-*b*-PDMS and PMMA-*g*-PDMS membranes at a DMS content of about 55 and 35 mol %, respectively. This suggests that the structural model for the permeation of an aqueous ethanol solution changes from a series model to a parallel model. Therefore, PMMA-*b*-PDMS membranes with over 55 mol % DMS and PMMA-*g*-PDMS membranes with over 35 mol % DMS have microphase separation characteristics corresponding to a parallel model. Furthermore, the PMMA2 phases showed a very small volume fraction in both PMMA-*b*-PDMS and PMMA-*g*-PDMS membranes at a DMS content of less than 55 and 35 mol %, respectively. This suggests that these membranes have a microphase separation corresponding to a series model. Therefore, the overall structural model for PMMA-*b*-PDMS and PMMA-*g*-PDMS membranes changes from a series model to a parallel model at a DMS content of 55 and 35 mol %, respectively.

On the basis of the discussion of the microphase separation in the combined model, it is easily understood that the PDMS phase changes from a discontinuous phase to a continuous phase in the direction of the membrane thickness at the corresponding DMS content. This suggestion is consistent with the aforementioned conclusion from the image processing. At a DMS content between 35 and 55 mol %, the differences in molecular architecture between the block and graft copolymers give rise to considerable differences in the morphology of the microphase separation. In other words, these results suggest that the PDMS component of the graft copolymer chains forms a continuous phase more readily than in block copolymer chains due to their molecular architecture. The PDMS segment length of both block

and graft copolymers may influence the morphology differences between the PMMA-*b*-PDMS and PMMA-*g*-PDMS membranes. We have observed the morphology of the PMMA-*g*-PDMS membranes having the pendant PDMS with various segment lengths. The PMMA-*g*-PDMS membranes having the same PDMS segment length as the block copolymers used in this study had a morphology similar to the PMMA-*g*-PDMS membranes used in this study. These suggest that the morphology differences between PMMA-*b*-PDMS and PMMA-*g*-PDMS membranes are mainly due to the architectural differences between a block and a graft structure. The PDMS segments in the graft copolymer membranes are probably assembled more quickly and easily than those of the block copolymer membranes because the former has a free PDMS segment end and the latter has both the PDMS segment ends fixed in the backbone chains. This must lead to a more stable microphase separation in the graft copolymer membranes than block copolymer membranes. In the block copolymer membranes, however, the fact that both the PDMS segment ends are fixed in the backbone may cause their well-defined morphology, i.e., bicontinuous phases. It is worth noting that both membranes changed from water- to ethanol-permselective at the DMS content corresponding to the change in the structural models. Consequently, these morphological changes can be directly related to the permselectivity for an aqueous ethanol solution through the PMMA-*b*-PDMS and PMMA-*g*-PDMS membranes during pervaporation.

Effects of Microphase Separation on Permselectivity. The aim of this study was to relate the permselectivity of two-component polymer membranes containing PDMS to their microphase separation by examining the morphology from various points of view. In particular, this study focuses on the difference in morphology between block and graft copolymer membranes. The results from the membrane morphology study led us to conclude that the microphase inversion takes place at the percolation point with a DMS content of about 55 and 35 mol % in the PMMA-*b*-PDMS and PMMA-*g*-PDMS membranes, respectively. At the percolation point in both membranes, the PDMS component changes from a discontinuous to a continuous phase, as shown in Figure 6. On the basis of the schematic model, the changes in the permselectivity of the PMMA-*b*-PDMS and PMMA-*g*-PDMS membranes can be explained as follows. Since the PMMA phase is rigid and has a high T_g , the diffusivity of the ethanol molecule must be lower than that of the water molecule in the PMMA phase because of its larger molecular size. As a result, the PMMA phase shows water-permselectivity in the separation of aqueous ethanol solutions during pervaporation, despite its stronger affinity for ethanol than for water.

In contrast, the PDMS phase is rubbery and has a very low T_g due to the rather free rotation of the siloxane bonds. It is well-known that the flexible PDMS chains and very high mobility of the permeant in the PDMS membrane result in its high permeability for gases and vapors.^{40–42} These unique properties of the PDMS phase must reduce difference in diffusivity between water and ethanol molecules; hence, they lead to an increase in the relative diffusivity of ethanol molecules. In addition, the PDMS chains have a relatively stronger affinity for the ethanol molecule than for the water molecule due to their hydrophobicity. Thus, the PDMS phase is

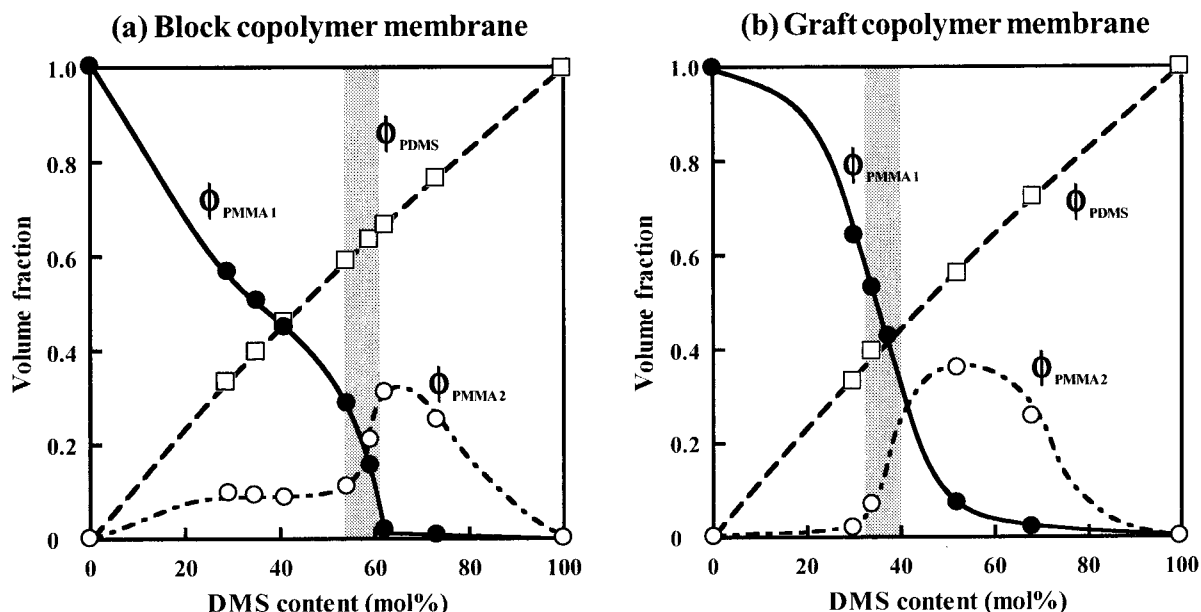


Figure 5. Relationship between the DMS content and the volume fraction of the elements in a combined model consisting of both a series model and a parallel model for PMMA-*b*-PDMS (a) and PMMA-*g*-PDMS (b) membranes: ●, volume fraction of the PMMA element in the series model (ϕ_{PMMA1}); ○, volume fraction of the PMMA element in the parallel model (ϕ_{PMMA2}); □, volume fraction of the PDMS element in the parallel model (ϕ_{PDMS}).

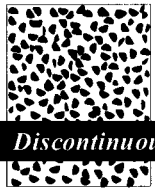





DMS content	Block copolymer membrane	Graft copolymer membrane
< 35 mol%	 Discontinuous → H ₂ O	 Discontinuous → H ₂ O
35 ~ 55 mol%	 Discontinuous → H ₂ O	 Continuous → EtOH
> 55 mol%	 Continuous → EtOH	 Continuous → EtOH

Figure 6. Tentative illustration of the relationship between the microphase separation in PMMA-*b*-PDMS and PMMA-*g*-PDMS membranes and their permselectivity for an aqueous ethanol solution.

ethanol-permselective for the permeation of aqueous ethanol solutions because of both high diffusivity and strong affinity. Consequently, the permselectivity of two-component polymer membranes containing PDMS and PMMA phases is strongly dependent upon the morphology of their microphase separation.

Percolation transition in graft copolymer membranes takes place at a lower DMS content than in block copolymer membranes, as the PDMS component in the former forms a continuous phase more readily than in the latter. In both block and graft membranes at a DMS content lower than the percolation point, the permeants

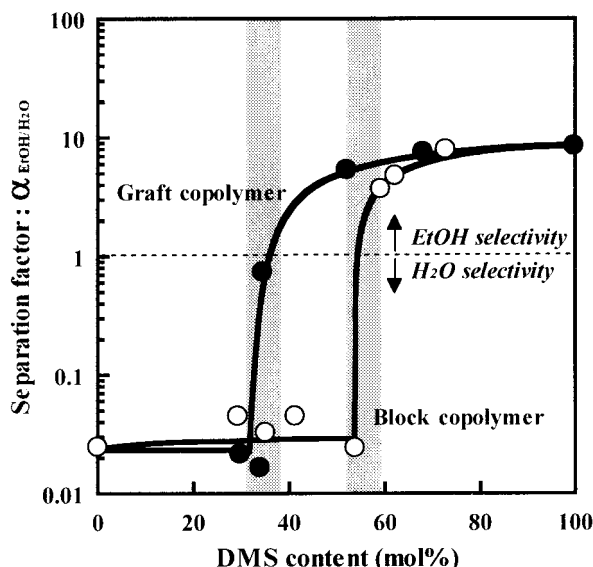


Figure 7. Separation factors for PMMA-*b*-PDMS (○) and PMMA-*g*-PDMS (●) membranes as a function of their DMS content. The separation factor is defined as $\alpha = (P_{\text{EtOH}}/P_{\text{H}_2\text{O}})/(F_{\text{EtOH}}/F_{\text{H}_2\text{O}})$, where P_i and F_i refer to the weight compositions of component i in the permeate and in the feed solution, respectively. A separation factor of less than one means a water-permselective membrane, whereas a factor greater than one represents an ethanol-permselective membrane.

are mainly diffusing in the continuous PMMA phase as the PDMS phase is discontinuous. The membranes then become water-permselective because the permselectivity of the membranes is strongly governed by the continuous PMMA phase. However, the PDMS component grows to form a continuous phase after the percolation transition takes place, and the permeants are preferentially diffusing in the continuous PDMS phase due to its high chain mobility and large free volume of PDMS. Both block and graft copolymer membranes then become ethanol-permselective because the permselectivity of the PDMS phase becomes more predominant than that of the PMMA phase. In addition, the fact that the highly permeable PDMS component changes from a discontinuous phase to a continuous phase gives rise to the dramatic increase in the permeability of the membranes at a DMS content over the percolation point. Consequently, the PMMA-*b*-PDMS and PMMA-*g*-PDMS membranes change from water- to ethanol-permselective at a DMS content of 55 and 35 mol %, respectively (Figure 7). The difference in the corresponding DMS content between the graft and block copolymer membranes can be attributed to their different molecular architecture. In particular, at a DMS content between 35 and 55 mol %, the remarkably different permselectivity between the PMMA-*b*-PDMS and PMMA-*g*-PDMS membranes suggests that membranes with differing molecular architecture exhibit different membrane characteristics, even if they have the same composition. The results of this study support the notion that designing the microphase separation of membranes via their molecular architecture is very important in controlling various membrane characteristics.

Conclusions

Two types of copolymer membranes, block and graft copolymer membranes, consisting of ethanol-permselective PDMS and water-permselective PMMA components were used to investigate the relationship between

their microphase separation and their permselectivity for aqueous ethanol solutions during pervaporation. With increasing DMS content, both the permeation rate and the ethanol concentration in the permeate increased. Similarly to the results reported in a previous paper, the PMMA-*g*-PDMS membranes changed from water- to ethanol-permselective at a DMS content of 35 mol %. However, the PMMA-*b*-PDMS membranes showed a dramatic change from water- to ethanol-permselectivity at a DMS content of 55 mol %. These membranes had a distinctive microphase separation consisting of a rubbery PDMS phase and a glassy PMMA phase. The morphology of the PMMA-*b*-PDMS membranes was quite different from that of the PMMA-*g*-PDMS membranes. It became apparent from TEM observations that the morphology of the microphase separation in the PMMA-*b*-PDMS membranes changed dramatically at a DMS content of about 55 mol %. A combined model consisting of parallel and series components suggested that the permeation of aqueous ethanol solutions through PMMA-*b*-PDMS membranes with a DMS content less than 55 mol % followed a series model, whereas permeation through membranes with a DMS content over 55 mol % changed to a parallel model. However, the PMMA-*g*-PDMS membranes changed from a series model to parallel model at a DMS content of about 35 mol %. Furthermore, image processing of the TEM micrographs demonstrated that the percolation transition of the PDMS phase in the PMMA-*b*-PDMS membranes occurred at a DMS content of about 55 mol %. These results led us to conclude that the PDMS component in PMMA-*b*-PDMS and PMMA-*g*-PDMS membranes changed from a discontinuous phase to a continuous phase at a DMS content of 55 and 35 mol %, respectively. The difference in the corresponding DMS content between the PMMA-*b*-PDMS and PMMA-*g*-PDMS membranes is likely due to their different molecular architecture. The dramatic morphological changes observed in their microphase separation resulted in both a drastic increase in the permeation rate and a change in the permselectivity. This study demonstrated that the permeability and permselectivity of multicomponent polymer membranes are strongly governed by the morphology of their microphase separation, which can be controlled by their molecular architecture. Designing the molecular architecture of membrane materials in order to control the morphology of their microphase separation is of great importance in the development of high-performance pervaporation membranes.

References and Notes

- (1) Huang, R. Y. M. *Pervaporation Membrane Separation Processes*; Elsevier: Amsterdam, 1991.
- (2) Takegami, S.; Yamada, H.; Tsujii, S. *J. Membr. Sci.* **1992**, *75*, 93.
- (3) Okamoto, S.; Butsuen, A.; Tsuru, S.; Nishioka, S.; Tanaka, K.; Kita, H.; Asaoka, S. *Polym. J.* **1987**, *19*, 747.
- (4) Ishihara, K.; Nagase, Y.; Matsui, K. *Makromol. Chem., Rapid Commun.* **1986**, *7*, 43.
- (5) Nagase, Y.; Mori, S.; Matsui, K. *J. Appl. Polym. Sci.* **1989**, *37*, 1259.
- (6) Nagase, Y.; Ishihara, K.; Matsui, K. *J. Polym. Sci., Polym. Phys. Ed.* **1990**, *28*, 377.
- (7) Nagase, Y.; Sugimoto, K.; Takamura, Y.; Matsui, K. *J. Appl. Polym. Sci.* **1991**, *43*, 1227.
- (8) Uragami, T.; Matsuda, T.; Nishimoto, H.; Miyata, T. *J. Membr. Sci.* **1994**, *88*, 243.
- (9) Uragami, T.; Kato, S.; Miyata, T. *J. Membr. Sci.* **1997**, *124*, 203.

- (10) Kempner, D.; Frisch, K. C. *Polymer Alloys III*; Plenum: New York, 1981.
- (11) Aggarwal, S. L. In *Processing, Structure and Properties of Block Copolymers*; Folkes, M. J., Ed.; Elsevier: New York, 1985; p 1.
- (12) Paul, D. R. In *Multicomponent Polymer Materials*; Paul, D. R., Sperling, L. H., Eds.; American Chemical Society: Washington, DC, 1986; p 3.
- (13) Prentice, P.; Papapostolou, E.; Williams, J. G. In *Multicomponent Polymer Materials*; Paul, D. R., Sperling, L. H., Eds.; American Chemical Society: Washington, DC, 1986; p 325.
- (14) Sperling, L. H. *Polymeric Multicomponent Materials*; John Wiley & Sons: New York, 1997.
- (15) Crank, J.; Park, G. S. *Diffusion in Polymers*; Academic Press: New York, 1968.
- (16) Barrie, J. A.; Munday, K. *J. Membr. Sci.* **1983**, *13*, 175.
- (17) Barrie, J. A.; William, M. J. L.; Spencer, H. *J. Membr. Sci.* **1984**, *21*, 185.
- (18) Barrie, J. A.; Sagoo, P.; Thomas, A. G. *J. Membr. Sci.* **1989**, *43*, 229.
- (19) Robeson, L. M.; Noshay, A.; Matzner, M.; Merriam, C. M. *Angew. Makromol. Chem.* **1973**, *29/30*, 47.
- (20) Barnabeo, A. E.; Creasy, W. S.; Robeson, L. M. *J. Polym. Sci., Polym. Chem. Ed.* **1975**, *13*, 1979.
- (21) Tsujita, Y.; Yoshimura, K.; Yoshimizu, H.; Takizawa, A.; Kinoshita, T. *Polymer* **1993**, *34*, 2597.
- (22) Fujimoto, T.; Ohkoshi, K.; Miyaki, Y.; Nagasawa, M. *J. Membr. Sci.* **1984**, *20*, 313.
- (23) Lerma, M. S.; Iwamoto, K.; Seno, M. *J. Appl. Polym. Sci.* **1987**, *33*, 625.
- (24) Chiou, J. S.; Paul, D. R. *J. Appl. Polym. Sci.* **1987**, *33*, 2935.
- (25) Lee, Y. K.; Tak, T.-M.; Lee, D. S.; Kim, S. C. *J. Membr. Sci.* **1990**, *52*, 157.
- (26) Lee, D. S.; Jung, D. S.; Kim, T. H.; Kim, S. C. *J. Membr. Sci.* **1991**, *60*, 233.
- (27) Lee, D. S.; Kang, W. K.; An, J. H.; Kim, S. C. *J. Membr. Sci.* **1992**, *75*, 15.
- (28) Kerres, J. A.; Strathmann, H. *J. Appl. Polym. Sci.* **1993**, *50*, 1405.
- (29) Miyata, T.; Takagi, T.; Kadota, T.; Uragami, T. *Macromol. Chem. Phys.* **1995**, *196*, 1211.
- (30) Miyata, T.; Takagi, T.; Uragami, T. *Macromolecules* **1996**, *29*, 7787.
- (31) Miyata, T.; Higuchi, J.; Okuno, H.; Uragami, T. *J. Appl. Polym. Sci.* **1996**, *61*, 1315.
- (32) Miyata, T.; Nakanishi, Y.; Uragami, T. *Macromolecules* **1997**, *30*, 5563.
- (33) Miyata, T.; Nakanishi, Y.; Uragami, T. *ACS Symp. Ser.*, in press.
- (34) Uragami, T.; Doi, T.; Miyata, T. *ACS Symp. Ser.*, in press.
- (35) Molau, G. E. In *Block Copolymers*; Aggarwal, S. L., Ed.; Plenum: New York, 1970.
- (36) Inoue, H.; Ueda, A.; Nagai, S. *J. Polym. Sci., Part A: Polym. Chem.* **1988**, *26*, 1077.
- (37) Inoue, H.; Ueda, A.; Nagai, S. *J. Appl. Polym. Sci.* **1988**, *35*, 2039.
- (38) Inoue, H.; Matsumoto, A.; Matsukawa, K.; Ueda, A. *J. Appl. Polym. Sci.* **1990**, *40*, 1917.
- (39) Trent, J. S.; Scheinbeim, J. I.; Couchman, P. R. *Macromolecules* **1983**, *16*, 589.
- (40) Plate, N.; Yampol'skii, Y. P. In *Polymeric Gas Separation Membranes*; Paul, D. R., Yampol'skii, Y. P., Eds.; CRC Press: London, 1994; p 155.
- (41) Kesting, R. E.; Fritzsche, A. K. *Polymeric Gas Separation Membranes*; John Wiley & Sons: New York, 1993.
- (42) Noll, W. In *Chemistry and Technology of Silicones*; Academic Press: New York, 1968.

MA981949X